blood

2012 119: 1844-1847
Prepublished online September 13, 2011;
doi:10.1182/blood-2011-07-365510

Reliable typing of systemic amyloidoses through proteomic analysis of subcutaneous adipose tissue

Francesca Brambilla, Francesca Lavatelli, Dario Di Silvestre, Veronica Valentini, Rossana Rossi, Giovanni Palladini, Laura Obici, Laura Verga, Pierluigi Mauri and Giampaolo Merlini

Blood (print ISSN 0006-4971, online ISSN 1528-0020), is published weekly by the American Society of Hematology, 2021 L St, NW, Suite 900, Washington DC 20036.

Brief report

Reliable typing of systemic amyloidoses through proteomic analysis of subcutaneous adipose tissue

*Francesca Brambilla,[1] *Francesca Lavatelli,[2,3] Dario Di Silvestre,[1] Veronica Valentini,[2] Rossana Rossi,[1] Giovanni Palladini,[2,4] Laura Obici,[2] Laura Verga,[5] Pierluigi Mauri,[1] and Giampaolo Merlini[2,4,6]

[1]Consiglio Nazionale delle Ricerche–Istituto Tecnologie Biomediche, Segrate, Milan, Italy; [2]Amyloid Research and Treatment Center, Fondazione Istituto di Ricovero e Cura a Carattere Scientifico Policlinico San Matteo, Pavia, Italy; [3]Biomedical Informatics Laboratory and [4]Department of Biochemistry, University of Pavia, Pavia, Italy; and [5]Department of Pathology and [6]Clinical Chemistry Laboratories, Fondazione Istituto di Ricovero e Cura a Carattere Scientifico Policlinico San Matteo, Pavia, Italy

Considering the important advances in treating specific types of systemic amyloidoses, unequivocal typing of amyloid deposits is now essential. Subcutaneous abdominal fat aspiration is the easiest, most common diagnostic procedure. We developed a novel, automated approach, based on Multidimensional Protein Identification Technology, for typing amyloidosis. Fat aspirates were obtained from patients with the most common systemic amyloidoses (ALλ, ALκ, transthyretin, and reactive amyloidosis), with Congo red score more than or equal to 3+, and nonaffected controls. Peptides from extracted and digested proteins were analyzed by Multidimensional Protein Identification Technology. On semiquantitative differential analysis (patients vs controls) of mass spectrometry data, specific proteins up-represented in patients were identified and used as deposit biomarkers. An algorithm was developed to classify patients according to type and abundance of amyloidogenic proteins in samples; in all cases, proteomic characterization was concordant with fibril identification by immunoelectron microscopy and consistent with clinical presentation. Our approach allows reliable amyloid classification using readily available fat aspirates. (*Blood*. 2012;119(8):1844-1847)

Introduction

Multiple unrelated autologous proteins can cause systemic amyloidoses.[1,2] The various forms differ for pathogenesis, prognosis, and treatment but present overlapping clinical manifestations, making their differentiation on a clinical basis very difficult. The most common type in Western countries is light chain (AL) amyloidosis, caused by misfolded monoclonal immunoglobulin light chains (LCs). However, several hereditary forms also exist, with high prevalence in selected geographic regions. Precise typing is key for adequate treatment because the various forms require different approaches, which can range from hematopoietic stem cell transplantation in AL amyloidosis to liver transplantation in transthyretin (TTR) amyloidosis (ATTR).[2] Diagnosis and classification are based on histologic demonstration of amyloid deposits and identification of which proteins originate the fibrils. Abdominal subcutaneous fat is the tissue of choice for diagnostic examination when a systemic form is suspected.[3] Because of the frequent unreliability of traditional, histochemistry-based typing techniques,[4-6] novel proteomic strategies, based on mass spectrometry (MS) identification of the protein constituents of the deposits, have been proposed.[7,8] Multidimensional Protein Identification Technology (MudPIT)[9,10] is an automated, high-throughput proteomic approach that allows identifying hundreds of proteins in complex samples.

We used MudPIT profiling for typing amyloid deposits in whole, nonfixed subcutaneous fat aspirates from patients affected by the most common forms of systemic amyloidoses: ALλ, ALκ, ATTR, and reactive (AA) amyloidosis. A simple diagnostic algorithm (α-value) was developed to use proteomic data for precise amyloid type assignment.

Methods

Subcutaneous abdominal fat was obtained by fine needle aspiration from 26 systemic amyloidosis patients (12 ALλ, 4 ALκ, 5 ATTR, and 5 AA) and 11 nonaffected controls (Table 1; supplemental Table 1, available on the *Blood* Web site; see the Supplemental Materials link at the top of the online article). Sample weight ranged between 10 and 20 mg both in patients (median, 12 mg) and controls (median, 15 mg). The use of the tissue for research purposes was approved by the Ethical Committee of Fondazione Istituto di Ricovero e Cura a Carattere Scientifico Policlinico San Matteo, Pavia, Italy. All persons gave written informed consent in accordance with the Declaration of Helsinki for storing and using their biologic samples for research purposes, according to the Institutional Review Board guidelines. Specific amyloidosis type was confirmed by immunoelectron microscopy (IEM), a reference method developed at our center.[13] All patients' samples had Congo red positivity score more than or equal to 3+.[11] Proteins were extracted from tissue as described,[7] dialyzed against 50mM ammonium bicarbonate (18 hours, 4°C), and digested with trypsin. Resulting peptide mixtures were analyzed in 2 replicates by MudPIT, based on 2-dimensional chromatography coupled to tandem MS.[14] The software MAProMa[14,15] was used to identify up-represented proteins in patients and select those forming

Submitted July 4, 2011; accepted August 30, 2011. Prepublished online as *Blood* First Edition paper, September 13, 2011; DOI 10.1182/blood-2011-07-365510.

*F.B. and F.L. contributed equally to this study.

There is an Inside *Blood* commentary on this article in this issue.

The online version of this article contains a data supplement.

The publication costs of this article were defrayed in part by page charge payment. Therefore, and solely to indicate this fact, this article is hereby marked "advertisement" in accordance with 18 USC section 1734.

Table 1. Clinical features, at time of fat tissue acquisition, of the 26 systemic amyloidosis patients included in the study

Sample	Amyloid type*	Age (y), sex	CR score†	Amyloid organ involvement‡	Serum MC (HR-IFE)	κ/λ ratio§
P1	AL-λ	61, F	3+	Kidney	IgGλ + λ-FLC	0.28
P2	AL-λ	53, M	3+	Heart, kidney	λ-FLC	0.05
P3	AL-λ	67, M	3+	Heart	IgGλ + λ-FLC	0.005
P4	AL-λ	59, F	3+	Heart, kidney, PNS, ANS	λ-FLC	0.06
P5	AL-λ	64, M	3+	Heart, kidney	IgAλ	0.009
P6	AL-λ	64, M	3+	Heart	λ-FLC	0.06
P7	ATTR (Val30Met)	68, M	3+	PNS		0.69
P8	AL-λ	68, F	3+	Heart, kidney, liver	λ-FLC	0.06
P9	AL-λ	58, M	3+	Heart, soft tissues	λ-FLC	0.03
P10	AL-λ	67, F	3+	Heart, kidney	IgAλ + λ-FLC	0.05
P11	AL-λ	73, F	3+	Heart, kidney, PNS	λ-FLC	0.05
P12	AL-λ	59, M	4+	Heart, kidney, PNS, ANS	λ-FLC	0.02
P13	AL-λ	70, F	4+	Kidney	IgMλ + λ-FLC	0.08
P14	AL-κ	75, M	4+	Heart, kidney, liver	κ- FLC + faint λ-FLC	7.7
P15	AL-κ	60, M	3+	Heart, soft tissues	κ-FLC + faint IgMλ	158
P16	ATTR (Tyr78Phe)	66, M	3+	Heart		0.64
P17	AA	70, F	3+	Kidney		0.48
P18	ATTR (Leu68Ile)	76, M	3+	Heart, PNS		1.31
P19	ATTR (Ser50Arg)	37, M	3+	Heart, PNS, ANS	IgAκ	2
P20	ATTR (Ser50Arg)	55, F	3+	Heart, PNS, ANS		0.94
P21	AA	70, M	4+	Kidney		1.08
P22	AA	75, F	4+	Kidney		1.4
P23	AA	66, F	4+	Kidney		1.33
P24	AA	79, M	3+	Kidney		1.62
P25	AL-κ	80, M	4+	Heart, soft tissues, PNS	IgGκ + κ-FLC	22.3
P26	AL-κ	63, M	4+	Kidney, PNS	IgGκ	21.8

CR indicates Congo red; MC, monoclonal component; HR-IFE, high-resolution electrophoresis and immunofixation; FLC, free light chains; PNS, peripheral nervous system; ANS, autonomic nervous system; LC-κ, immunoglobulin light chain-κ; and LC-λ, immunoglobulin light chain-λ.

*Confirmed by IEM.

†Graded on subcutaneous fat tissue.[11]

‡Defined according to the International Consensus Panel criteria.[12]

§Reference interval: 0.26-1.65.

the amyloid deposits in each amyloidosis type, by comparing each patient's fat sample protein profile against the profile of the same tissue from the nonaffected population. For estimating which specific amyloid protein was prevalent in each patient, a parameter (α-value) was calculated; this is obtained by normalizing the patient over control ratio of each biomarker's spectral count[16] (further details in supplemental Methods).

Results and discussion

MudPIT allowed identifying hundreds of proteins in each fat sample, among which a few carried over serum proteins (supplemental Table 2). Protein profiles from amyloidosis patients were compared against that of the control counterpart; this allowed minimizing the contribution of contaminating blood proteins and selecting up-represented proteins in patients. Within each of the 4 considered groups of patients (clustered by amyloidosis type), only a single amyloidogenic protein was up-represented in 100% of cases. These 4 proteins (LC λ, LC κ, TTR, and serum amyloid A [SAA]), identified by proteomic analysis, matched those expected to constitute the fibrils according to IEM (Figure 1; supplemental Table 3). In addition, other proteins (supplemental Table 3) were found to be over-represented across the various amyloidoses, including clusterin,[17] apolipoprotein E,[18,19] apolipoprotein A-IV,[20] vitronectin,[18] basement membrane-specific heparan sulfate proteoglycan core protein,[21] sushi-repeat-containing protein, and serum amyloid P.[22] Most of these had previously been described as associated with amyloid fibrils and involved in the mechanisms of amyloid formation; this confirms that MudPIT can fully characterize the deposits in whole adipose tissue and constitutes an internal validation parameter. In addition, sushi-repeat–containing protein may play a role in amyloid disease; indeed, it is secreted by adipocytes[23] and may intervene in adipogenic differentiation,[24] regulation of body weight, and metabolism.[24,25] Moreover, evidence of its involvement in tumor suppression, possibly through apoptosis induction,[26] emphasizes its potential interest in amyloid cell toxicity. However, its potential role may be limited to subcutaneous fat because it has not been reported in other studies on amyloid.

The 4 amyloid proteins identified by MS in the previous step (LC λ, LC κ, TTR, and SAA), specific for each amyloidosis type, were used to design a diagnostic algorithm, based on calculation of the parameter α-value (Figure 2; supplemental Methods). α-value allows to estimate the abundance of each amyloid protein relative to the remaining ones, eliminating the confounding effect of carried-over LC, SAA, and TTR from blood (Figure 1). The diagnostic capability of the algorithm was tested by assigning in blind the amyloid type to the aforedescribed patients. The α-values of each of the 4 amyloid proteins were calculated for all patients; amyloid was assigned to the type whose amyloid protein α-value was predominant. In all cases, amyloid-type definition according to α-value was in agreement with IEM and could be visualized in a user-friendly graphical representation (Figure 2). Notably, disease classification was correct also in the 2 AL amyloidosis patients (P14 and P15) who had biclonal gammapathies (P14, both κ- and λ-free LC bands; P15, κ-free LC and IgMλ bands), and in the ATTR patient (P19) with a coincidental serum IgAκ monoclonal component. The observation that, in cases such as P9 and P13, minor amounts of other amyloid proteins (TTR and κ LC,

		Dave/DCI (Patients vs Controls)				Spectral Count			
Sample	Diagnosis *	LC κ	LC λ	TTR	SAA	LC κ	LC λ	TTR	SAA
P6		0.82/670	1.70/7800	0	0	13	212	6	6
P11		0	1.52/2783	0	0	6	165	4	0
P2		0	1.32/1210	0	0	0	130	0	0
P1		0	1.55/3171	0	0	0	88	6	0
P9		0.64/412	1.63/4975	1.21/1436	0	13	61	9	0
P12	ALλ	0	1.38/1476	0	0	8	50	0	0
P13		0	1.33/1229	0	0	14	34	0	0
P8		0	1.65/5488	0	0	7	33	0	0
P4		0	0.99/405	0	0	0	22	0	0
P3		0	1.26/972	0	0	0	21	0	0
P5		0	1.37/1466	0	0	0	13	0	0
P10		0	0.99/412	0	0	0	6	0	0
P15		1.61/12077	0	0	0	372	0	0	0
P14	ALκ	1.34/3582	0	0	0	176	0	0	0
P25		0.99/1121	0	0	0	44	0	0	0
P26		0.70/486	0	0	0	14	0	0	0
P19		0	0	1.91/164844	0	4	0	1158	0
P20		0	0	1.78/28540	0	0	0	185	0
P16	ATTR	0	0	1.56/5990	0	4	0	145	0
P18		0	0	1.58/6556	0	0	0	89	0
P7		0	0	0.86/496	0	4	0	16	0
P22		0	0	0	1.1/569	0	0	0	638
P23		0	0	0	1.78/15322	0	0	0	261
P17	SAA	0.81/666	0	0	1.49/2416	10	0	0	166
P24		0	0	0	1.61/4487	0	0	0	93
P21		0	0	0	1.49/2346	0	0	0	71
Cm		-	-	-	-	4	2	1	1
Color legend		0	1-2	3-5	6-9	10-19	20-29	30-49	>50

Figure 1. Amyloid proteins detected by proteomics analysis in patients' abdominal subcutaneous fat tissue. Results of semiquantitative differential analysis (patients vs controls) and absolute spectral count of the amyloid proteins are shown. Specific amyloid proteins were identified by comparing the protein lists of each patient against the average protein profile of nonaffected adipose tissue, by means of MAProMa software (through calculation of Dave/DCI values; Dave ≥ +0.4 and DCI ≥ +400 correspond to proteins significantly up-represented in patients).[14] For LC-κ and LC-λ, the contributions of both constant and variable regions were considered. SAA indicates serum amyloid A; Cm, the average value of each amyloid protein in nonaffected tissue, acquired from 11 controls and deposited in our database; and —, not applicable. *Confirmed by IEM.

respectively) were identified in conjunction with λ LC indicates the possibility that "normal" proteins can adsorb on amyloid fibrils. Combining MudPIT with complementary approaches, such as laser capture microdissection or IEM, would determine whether these proteins colocalize with fibrils.

Our technique was developed in patients with clear-cut amyloid deposits (Congo red score 3+/4+). In AL and AA samples with 1+/2+ amyloid, the MudPIT approach may not allow conclusive typing. In these cases, enrichment of amyloid areas by laser capture microdissection before MS, proposed by Vrana et al,[8] may be necessary.

The described method is a novel approach for diagnostic amyloid typing in whole unfixed adipose tissue, coupling the advantages of using subcutaneous abdominal fat aspirates (ease of acquisition, wide applicability) with the automation and sensitivity of MudPIT. Analysis of whole tissue avoids fractionation steps, and the inclusion of the control group compensates for the background noise of carried-over plasma proteins. MS-based amyloid typing was concordant with IEM, validating the correctness of the results. Although thus far only implemented for the 4 described amyloid types, the approach can be expanded to the diagnosis of other forms. A limitation is that, in some types of systemic amyloidosis, particularly ATTR and ApoA-I, amyloid deposits may be scanty or absent in abdominal fat. In these cases, biopsy of involved organs, analyzed by laser capture microdissection and MS,[8] is necessary. It has been argued that direct MS-based approaches for protein identification and quantification are less prone to biases than antibody-based methods, especially for proteins with altered conformation as amyloid ones. Our results indicate this method as a specific and informative novel potential diagnostic approach, granting its application on larger, independent patient sets, possibly through a multicenter collaboration.

Acknowledgments

This work was supported by the Fondazione Cariplo Nobel project, Proteomic platform, Operational Network for Biomedicine Excellence in Lombardy, EURAMY project (Community's Sixth Framework Program), Fondazione Cariplo (N2009-2532), Ricerca Finalizzata Malattie Rare, Italian Ministry of Health, Istituto Superiore di Sanità (526D/63), Ministry of Research and University (2007AESFX2-003), and Associazione Italiana per la Ricerca sul Cancro Special Program Molecular Clinical Oncology (grant 9965).

Authorship

Contribution: F.B. wrote the manuscript, performed MudPIT analysis, and interpreted results; F.L. wrote the manuscript, processed tissue samples, collected clinical data, and interpreted

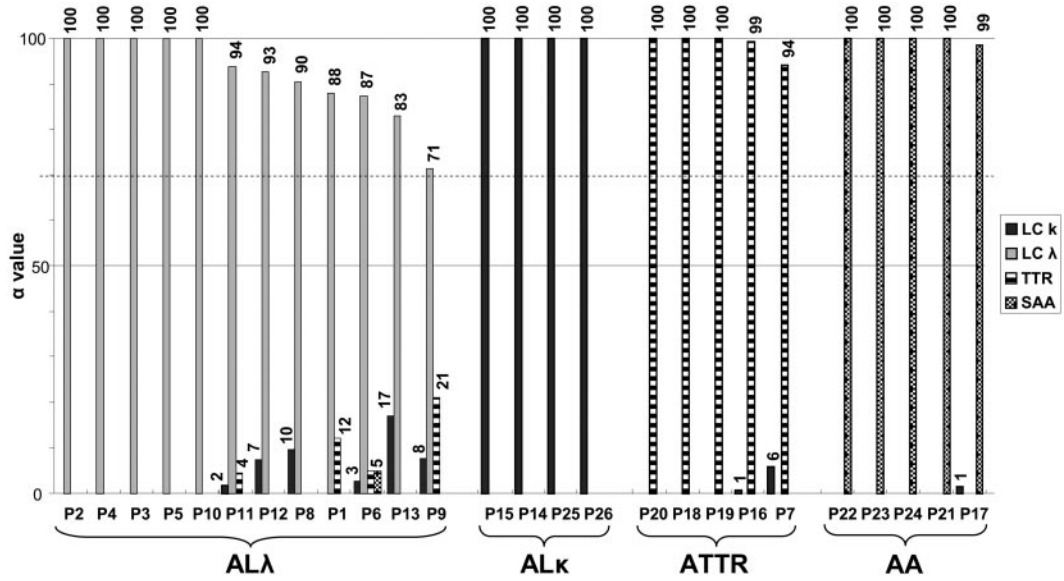

Figure 2. Typing of systemic amyloidosis through MS-based diagnostic algorithm in 26 patients. Bars in the graph represent the α-values of the 4 amyloid proteins in each patient. α-value is the normalized patient over control ratio of each amyloid protein's spectral count (see supplemental Methods). Amyloidosis is attributed to the type whose corresponding amyloid protein has the highest α-value. Discontinuous line indicates the theoretical diagnostic threshold (α-value = 70; see supplemental Methods). Based on this algorithm, all patients were correctly classified (ie, amyloid-type definition was in accordance with IEM).

results; D.D.S. and R.R. performed MudPIT analysis and interpreted results; V.V. processed tissue samples; G.P. and L.O. collected samples and clinical data; L.V. performed IEM; P.M. designed research, developed the algorithm for α-value, and revised the manuscript; and G.M. designed research, collected clinical data, and revised the manuscript.

Conflict-of-interest disclosure: The authors declare no competing financial interests.

Correspondence: Giampaolo Merlini, Amyloid Research and Treatment Center, Fondazione IRCCS Policlinico San Matteo and University of Pavia, Viale Golgi 19, 27100 Pavia, Italy; e-mail: gmerlini@smatteo.pv.it.

References

1. Merlini G, Seldin DC, Gertz MA. Amyloidosis: pathogenesis and new therapeutic options. *J Clin Oncol.* 2011;29(14):1924-1933.
2. Obici L, Perfetti V, Palladini G, Moratti R, Merlini G. Clinical aspects of systemic amyloid diseases. *Biochim Biophys Acta.* 2005;1753(1):11-22.
3. Westermark P, Davey E, Lindbom K, Enqvist S. Subcutaneous fat tissue for diagnosis and studies of systemic amyloidosis. *Acta Histochem.* 2006; 108(3):209-213.
4. Picken MM, Herrera GA. The burden of "sticky" amyloid: typing challenges. *Arch Pathol Lab Med.* 2007;131(6):850-851.
5. Solomon A, Murphy CL, Westermark P. Unreliability of immunohistochemistry for typing amyloid deposits. *Arch Pathol Lab Med.* 2008;132(1): 14.
6. Lachmann HJ, Booth DR, Booth SE, et al. Misdiagnosis of hereditary amyloidosis as AL (primary) amyloidosis. *N Engl J Med.* 2002;346(23):1786-1791.
7. Lavatelli F, Perlman DH, Spencer B, et al. Amyloidogenic and associated proteins in systemic amyloidosis proteome of adipose tissue. *Mol Cell Proteomics.* 2008;7(8):1570-1583.
8. Vrana JA, Gamez JD, Madden BJ, Theis JD, Bergen HR 3rd, Dogan A. Classification of amyloidosis by laser microdissection and mass spectrometry-based proteomic analysis in clinical biopsy specimens. *Blood.* 2009;114(24):4957-4959.
9. Washburn MP, Wolters D, Yates JR 3rd. Large-scale analysis of the yeast proteome by multidimensional protein identification technology. *Nat Biotechnol.* 2001;19(3):242-247.
10. Mauri P, Scigelova M. Multidimensional protein identification technology for clinical proteomic analysis. *Clin Chem Lab Med.* 2009;47(6):636-646.
11. Hazenberg BP, Bijzet J, Limburg PC, et al. Diagnostic performance of amyloid A protein quantification in fat tissue of patients with clinical AA amyloidosis. *Amyloid.* 2007;14(2):133-140.
12. Gertz MA, Comenzo R, Falk RH, et al. Definition of organ involvement and treatment response in immunoglobulin light chain amyloidosis (AL): a consensus opinion from the 10th International Symposium on Amyloid and Amyloidosis, Tours, France, 18-22 April 2004. *Am J Hematol.* 2005; 79(4):319-328.
13. Arbustini E, Verga L, Concardi M, Palladini G, Obici L, Merlini G. Electron and immuno-electron microscopy of abdominal fat identifies and characterizes amyloid fibrils in suspected cardiac amyloidosis. *Amyloid.* 2002;9(2):108-114.
14. Mauri P, Deho G. A proteomic approach to the analysis of RNA degradosome composition in Escherichia coli. *Methods Enzymol.* 2008;447:99-117.
15. Regonesi ME, Del Favero M, Basilico F, et al. Analysis of the Escherichia coli RNA degradosome composition by a proteomic approach. *Biochimie.* 2006;88(2):151-161.
16. Liu H, Sadygov RG, Yates JR 3rd. A model for random sampling and estimation of relative protein abundance in shotgun proteomics. *Anal Chem.* 2004;76(14):4193-4201.
17. Greene MJ, Sam F, Soo Hoo PT, Patel RS, Seldin DC, Connors LH. Evidence for a functional role of the molecular chaperone clusterin in amyloidotic cardiomyopathy. *Am J Pathol.* 2011; 178(1):61-68.
18. Gallo G, Wisniewski T, Choi-Miura NH, Ghiso J, Frangione B. Potential role of apolipoprotein-E in fibrillogenesis. *Am J Pathol.* 1994;145(3):526-530.
19. Klein CJ, Vrana JA, Theis JD, et al. Mass spectrometric-based proteomic analysis of amyloid neuropathy type in nerve tissue. *Arch Neurol.* 2011;68(2):195-199.
20. Bergstrom J, Murphy C, Eulitz M, et al. Codeposition of apolipoprotein A-IV and transthyretin in senile systemic (ATTR) amyloidosis. *Biochem Biophys Res Commun.* 2001;285(4):903-908.
21. Elimova E, Kisilevsky R, Szarek WA, Ancsin JB. Amyloidogenesis recapitulated in cell culture: a peptide inhibitor provides direct evidence for the role of heparan sulfate and suggests a new treatment strategy. *FASEB J.* 2004;18(14):1749-1751.
22. Pepys MB, Rademacher TW, Amatayakul-Chantler S, et al. Human serum amyloid P component is an invariant constituent of amyloid deposits and has a uniquely homogeneous glycostructure. *Proc Natl Acad Sci U S A.* 1994; 91(12):5602-5606.
23. Rosenow A, Arrey TN, Bouwman FG, et al. Identification of novel human adipocyte secreted proteins by using SGBS cells. *J Proteome Res.* 2010;9(10):5389-5401.
24. Celebi B, Elcin AE, Elcin YM. Proteome analysis of rat bone marrow mesenchymal stem cell differentiation. *J Proteome Res.* 2010;9(10):5217-5227.
25. Dahlman I, Linder K, Arvidsson Nordstrom E, et al. Changes in adipose tissue gene expression with energy-restricted diets in obese women. *Am J Clin Nutr.* 2005;81(6):1275-1285.
26. Pawlowski K, Muszewska A, Lenart A, Szczepinska T, Godzik A, Grynberg M. A widespread peroxiredoxin-like domain present in tumor suppression- and progression-implicated proteins. *BMC Genomics.* 2010;11:590.